Determination of the Electron's Atomic Mass and the Proton/Electron Mass Ratio via Penning Trap Mass Spectroscopy

Dean L. Farnham, Robert S. Van Dyck, Jr., and Paul B. Schwinberg
Department of Physics, University of Washington, Box 351560, Seattle, Washington 98195-1560
(Received 14 June 1995)

Accuracy of the electron's atomic mass has been improved tenfold by comparing cyclotron frequencies of electrons and single C^{6+} ions alternately confined to the same uniform magnetic field in a Penning trap. Cyclotron resonances are observed via frequency shifts in the particle's continuously monitored harmonic motion parallel to the field. Field instability and relativity cause, respectively, the leading statistical and systematic errors. Combining the electron's atomic mass $M_e = 0.000\,548\,579\,911\,1(12)$ u with the proton's yields the mass ratio $m_p/m_e = 1836.152\,666\,5(40)$.

PACS numbers: 06.20.Jr, 07.75.+h, 14.60.Cd, 32.10.Bi

A 10 times more accurate measurement of the electron's atomic mass M_e has yielded a new value for the proton-to-electron mass ratio m_p/m_e. Precise determination of m_p/m_e is essential for the experimental determination of other fundamental physical constants, providing a necessary link between tests of physical theories and the analysis of experimental data. As such, m_p/m_e and M_e represent important key inputs for the periodic least squares adjustment of the fundamental constants [1]. Increased accuracy has become crucial for maintaining the status of m_p/m_e, previously elevated from adjusted parameter to input constant, in the next adjustment [2] and for extending the determination of other constants such as the Rydberg from the analysis of hydrogen spectra [3,4] and the fine-structure constant from measurements of Compton wavelengths [2,5,6].

Direct determinations of m_p/m_e compare the cyclotron frequencies of electrons and protons in a uniform magnetic field, B_0. The first such precise determination [7] in 1978 began the fruitful use [8–11] of the electrostatic quadrupole field of a Penning trap to alternately confine these particles to the same small region of B_0. Since that time, a 10^3-fold improvement in precision has gradually been realized, exceeding by a factor of 150 the best *indirect* determination [12] obtained by measuring the electron g_j factor of $^9Be^+$ ions confined in a Penning trap.

For our new measurement, the cyclotron frequency of the electron $\omega_c = eB_0/m_e$, where e is the elementary charge, is compared not with ω_c of the proton but with that of a single trapped C^{6+} ion. Comparison to the neutral carbon is attained by correcting the ion mass for the removed electrons and their binding energies, assuming that the free electron's charge and rest mass remain unchanged when bound to a nucleus. This yields the electron's mass in unified atomic mass units u. The proton's atomic mass, similarly measured by others, has an accepted value [13] $m_p = 1.007\,276\,466\,6(6)$ u with accuracy sufficient to not limit this m_p/m_e determination.

Extensive descriptions of the University of Washington Penning trap mass spectrometer (UW-PTMS) are available [14–16]. Our unique nondestructive rf detection of the particles in the Penning trap is possible because the quadrupole field produces harmonic confinement in the axial direction (parallel to $\vec{B}_0$). The main electrodes, a ring and two end caps, are chosen to be hyperboloids of axial revolution in order to minimize all anharmonic terms in the electric field. In addition, a pair of compensation or guard ring electrodes [17] allow significant further reduction and control of the remaining anharmonicity in the trap so that the frequency of the axial motion $\omega_z = 2\pi\nu_z = \sqrt{qV_0/md^2}$ may be resolved to better than 10 ppb (10 parts in 10^9), limited by the stability of the end-cap-to-ring potential V_0. Here, q/m is the charge-to-mass ratio of the confined particle and $d = 2.1$ mm is the characteristic trap dimension. For our trap, $\nu_z = 95$ or 142 MHz for the electron (with $V_0 = 9.3$ or 20.5 V), and $\nu_z \sim 4$ MHz for C^{6+} (with $V_0 = 57.5$ V).

The quadrupole electric field modifies the cyclotron motion so that it has the observed frequency $\omega_c' = \omega_c - \omega_m$, where ideally $\omega_m = \omega_z^2/2\omega_c'$. However, the unmodified cyclotron frequency ω_c is actually determined from the three observable frequencies via

$$(\omega_c)^2 = (\omega_c')^2 + (\omega_z)^2 + (\omega_m)^2, \qquad (1)$$

which is valid [18] in spite of a possible misalignment between the magnetic and electric field axes and certain other electrode imperfections. In the 5.8 T magnetic field of our superconducting solenoid $\omega_c'/2\pi$ is ~164 GHz for the electron and ~45 MHz for C^{6+}.

Changes in the state of the trapped particle are monitored entirely through small frequency shifts in its axial motion. This motion induces currents at ω_z which, detected as a voltage across a cryogenically cooled tuned circuit with $Q \sim 500 - 1100$, damp the motion. A coherently driven motion smaller than the thermal motion is observed by setting the detection bandwidth narrower than the damped axial linewidth. And frequency shifts in ω_z are observed as a phase difference between the detected signal and the coherent drive. By adding the integrated phase-difference signal to the trapping potential V_0, the particle's axial motion is frequency locked to

 0031-9007/95/75(20)/3598(4)$06.00

the drive frequency. This not only stabilizes ω_z and ω_m for Eq. (1), but also provides a "frequency-shift signal," giving information about small perturbations to ω_z which arise from excitation of the cyclotron motion.

Magnetic, relativistic, and electrostatic couplings of the axial frequency to the cyclotron energy E_c result in frequency shifts which, to leading order in the small quantity $\alpha = \omega_z/\omega_c'$, are (adapted from Ref. [19])

$$\frac{\delta\omega_z}{\omega_z} = \left[\frac{B_2}{m\omega_z^2 B_0} - \frac{1}{2mc^2} - \frac{3C_4\alpha^2}{qV_0}\right]E_c . \quad (2)$$

Here, B_2 is the "magnetic bottle" coefficient describing the residual quadratic gradient in the magnetic field, and C_4 is the coefficient describing the leading order anharmonic correction to the quadrupole potential. The very useful B_2 coupling has limited the accuracy of previous measurements [10] by making the cyclotron frequencies of the two particles slightly orbit position dependent. Consequently this coupling has been minimized ($B_2 = 1.4$ G/cm^2) and presents no current limitation.

The ion mass is too large for the relativistic shift in ω_z [second term in Eq. (2)] to render a useful cyclotron resonance signal. However, C_4 may be increased (via the guard electrodes) from its minimum in our trap (3×10^{-6}) to (typically) -3×10^{-5} for anharmonic detection [20] without seriously impacting the axial frequency resolution. For C^{6+}, Eq. (2) then yields $\delta\omega_z/\omega_z \simeq (5.2\ \text{ppb/eV})E_c$ (where ppb denotes parts per 10^9), or a detection threshold of $\Delta E_c \simeq 2$ eV.

In contrast, the relativistic term in Eq. (2) is quite useful for detecting E_c of the less massive electron, whereas the C_4 term is not (α^2 is $\sim 10^4$ times smaller). For electrons, Eq. (2) yields $\delta\omega_z/\omega_z = (-930\ \text{ppb/eV})E_c$, corresponding to a detection threshold of $\Delta E_c = 10$ meV.

The couplings which give rise to the axial-frequency-shift signal also perturb the cyclotron frequency, altering the line shapes and potentially causing systematic errors. Effects of changing the well depth V_0 (to keep ω_z locked) must also be included to correctly describe these shifts and line shapes. The result [21] (to leading order in α) is

$$\frac{\delta\omega_c'^{\text{lock}}}{\omega_c'} = \left[-\frac{1}{mc^2} - \frac{3C_4\alpha^4}{2qV_0}\right]E_c + \left[\frac{2B_2}{m\omega_z^2 B_0} + \frac{\alpha^2}{mc^2}\right]E_m + \left[\frac{B_2}{m\omega_z^2 B_0} - \frac{1}{2mc^2} - \frac{3C_4\alpha^2}{2qV_0}\right]E_z , \quad (3)$$

where E_z and E_m are the axial and magnetron energies. The E_c term results in a pulling of the cyclotron frequency in which the relativistic effects dominate the C_4 term by at least an order of magnitude *even* for the massive C^{6+} under our conditions for anharmonic detection.

The effect of this relativistic pulling is seen in the shape of the single C^{6+} cyclotron resonance in Fig. 1. The abrupt step response with the up-frequency sweep of the excitation drive occurs when energy absorption causes the resonance to be pulled through to the lower side of the drive. When sweeping the drive down in frequency, the response is a straight sloping line as energy absorption shifts ω_c' so that it remains just below the drive. The undisturbed cyclotron resonance (at the frequency of the *initial* responses) can be resolved to ± 0.5 ppb. In this trap, the guard electrodes are split for application of the rf ion cyclotron drive. Between each sweep, the cyclotron energy is removed (in ~ 1 min) by applying to the split guards, a sideband drive at $\omega_c' - \omega_z$ which couples [15] the cyclotron motion to the strongly damped axial resonance.

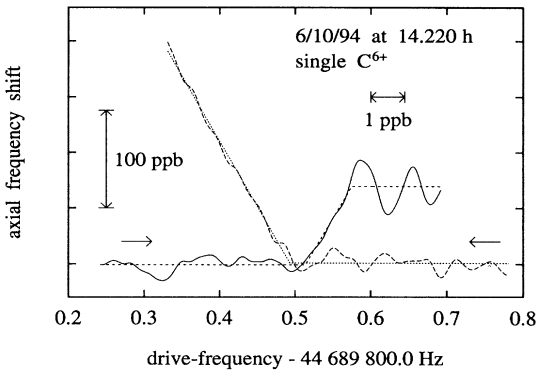

FIG. 1. Single C^{6+} cyclotron resonance via anharmonic detection. Such pairs of up- and down-frequency sweeps are taken every 3–4 min via computer. The fitted line segments aid in determining the frequency of the initial response.

The cyclotron motion of the electron is at a frequency such that it is strongly damped ($\sim$80 msec lifetime) by synchrotron radiation. Therefore, while the response of the *single* electron to a down-swept cyclotron drive appears similar to that of the C^{6+}, no step typical of the undamped ion is seen for an up-frequency sweep. Another consequence of the pulling of Eq. (3) for the *single* electron is that ω_c' is shifted by amounts approaching -20 ppb before Eq. (2) gives rise to an identifiable shift in ω_z. One can determine the unshifted cyclotron resonance by simply extrapolating the observed pulling (for detectible E_c) back to the zero-axial-frequency-shift baseline. However, the single "pull" resolution of ~ 15 ppb requires too many such pulls for adequate determination of w_c'.

Most of the electron ω_c data were taken using small clouds of 5–13 electrons, since they provided the necessary ($\sim$8 times) improved resolution. The cyclotron motion is much more strongly damped for these clouds due, in part, to the collisional transfer of E_c to the axial motion. Consequently E_c remains small and the axial-frequency-shift signal of Eq. (2) disappears. However, the change in axial energy ΔE_z may be detected via

$$\frac{\delta\omega_z}{\omega_z} = \left[-\frac{3}{8mc^2} + \frac{3C_4}{2qV_0}\right]E_z \quad (4)$$

(again to leading order) with the anharmonicity increased to typically $C_4 = -3 \times 10^{-4}$. This yields a detection threshold of $\Delta E_z = 0.45$ meV, corresponding to an axial temperature change of $\Delta T_z = 5$ K. The pulling of ω_c',

strongly dominated now by *both* (E_c and E_z) relativistic terms of Eq. (3), is still extrapolated to zero shift. However, the extrapolation for these clouds is small since the shift at the detection threshold is $\delta\omega_c'/\omega_c' \sim -0.8$ ppb.

Unlike the single electron, the cloud resonance of Fig. 2 shows a response when the drive is swept up in frequency because the cyclotron line now demonstrates a width which is larger than the pulling at the onset of detection. The resonance is pulled through the up-swept drive when it approaches within the linewidth, accounting for the sharp response. The resonance width (which has been reduced to ~6 ppb on one occasion, and for comparison is ~0 for C^{6+} in Fig. 1) is defined as the frequency interval between the sharp up-sweep response and the extrapolation of the down-sweep pull to the zero-axial-frequency-shift baseline. Expecting a symmetric unpulled line shape, the resonance center is taken to be the midpoint of this frequency interval. This choice is experimentally justified by the independence of the center frequency on the observed width and the (typically ± 1 ppb) agreement with single-electron cyclotron resonances. We find the resonance width is not affected by moderate changes (6–12 dB) in the strength of the axial drive, the anharmonicity ($-0.0014 \leq C_4 \leq +0.0013$), the number of particles in the cloud (5–30) when properly cooled, or small B field gradients. The width does depend strongly on the microwave drive power, as demonstrated by Fig. 3. However, the independence (within ± 1 ppb) of the line center on the width is also shown. Power broadening occurs symmetrically about the center of the line, which is also found to be independent (within ± 1) of the same changes in C_4, and particle number.

Corrections to ω_c must be made for the finite energies E_c, E_z, and E_m before the E_c excitation. The *dominant* terms in these corrections [21] are the same (to leading order in α) as in Eq. (3), i.e., $\delta\omega_c/\omega_c \simeq \delta\omega_c^{\text{lock}}/\omega_c'$.

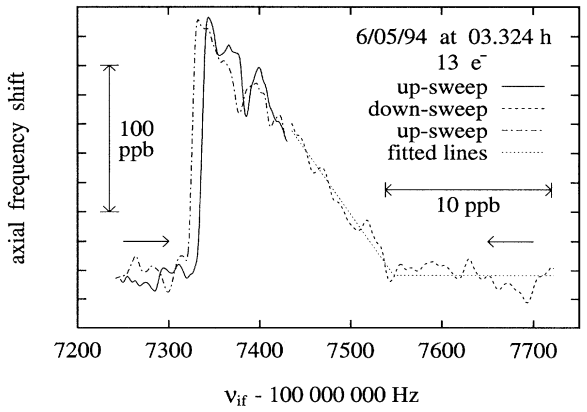

FIG. 2. Small electron cloud cyclotron resonance. Three consecutive sweeps of the microwave drive at 162.623 GHz + $9(\nu_{if})$ are shown, the up sweeps bracketing (in time) the down sweep. The linear pulling response with the down sweep would continue past the sharp up-sweep response if the drive were to be swept down that far.

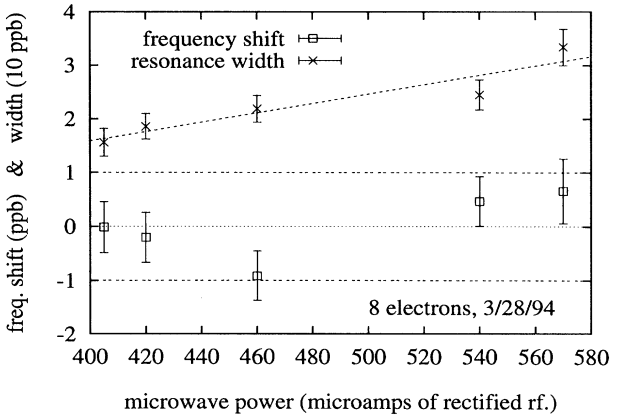

FIG. 3. Drive power dependence of the frequency and width of the small electron cloud cyclotron resonance. While the width of the resonance is seen to change by a factor of ~2, the center of the resonance remains fixed to within ± 1 ppb over the 3 dB range of the abscissa.

For electrons, relativity causes the required corrections. A typical E_m of ~ -30 μeV produces an insignificant shift. The electron cyclotron radiative coupling to the 4.2 K environment results in an average energy before excitation of $E_c = 0.68\hbar\omega_c' = 460$ μeV for which a systematic correction of $\delta\omega_c/\omega_c = +0.90$ ppb is applied. Uncertainty in E_c of the cloud (due to the particle number dependent collisional coupling to E_z) is represented in our error budget (Table I) by the ± 1 ppb uncertainty in the number dependence and agreement with the single electron resonances. The temperature of the axial motion would also be 4.2 K if it were not for the preamplifier which heats E_z to a measured 1 ± 0.7 meV (12 ± 8 K), requiring a correction of $\delta\omega_c/\omega_c = +1 \pm 0.7$ ppb. No correction is necessary for the clouds' random spin states. For the ion, typical E_c, E_z, and E_m cause insignificant shifts ($\delta\omega_c/\omega_c \ll 0.1$ ppb). A correction of +0.3 ppb is applied for the ion's electrostatic image charge shift [22].

Figure 4 represents data of a typical run. Residual field variations require data to be taken over a period long enough to establish the average ~0.2 ppb/h magnetic field drift and ω_c ratio. Here, three days of C^{6+} data are compared with 2 d of data from small clouds of 6–10 electrons. Correcting the simple average of our six runs for the systematic errors as shown in Table I yields

$$\omega_c(C^{6+})/\omega_c(e^-) = 0.000\,274\,365\,185\,89(28)\,. \quad (5)$$

The 1σ error bar in Eq. (5) is the statistical distribution (due to field instability) of the six run average.

Effects of magnetic field gradients deserve particular attention. Using an NMR probe, the magnetic field uniformity has been shown to be better than 80 ppb/cm *without* the trap. The cylindrically symmetric trap apparatus can only change the axial gradients B_1, B_2, etc., and broken axial reflection symmetry induces a linear gradient $B_1/B_0 \simeq 24$ ppb/cm before correcting with a pair of cylindrically symmetric shim coils. When B_1 was reduced by a factor of ~220 (to $B_1/B_0 \simeq 110$ ppb/cm),

TABLE I. Systematic corrections and error budget.

Source of error	Correction ± error in Eq. (5) (ppb)
Electron:	
Cloud number dependence	0 ± 1.0
Cloud line splitting (cloud vs single)	0 ± 1.0
Cyclotron drive power, single or clouds	0 ± 1.0
Cyclotron energy (ambient, relativistic)	−0.9 ± (≪1.0)
Axial energy (driven, relativistic)	−1.0 ± 0.7
Spin state (statistical, relativistic)	0 ± (≪1.0)
Carbon	
Image charge shift	0.3 ± (≪1.0)
Electron and carbon	
$\vec{B}$ field instability (statistical)	0 ± 1.0
$\vec{B}$ field gradients (B_1, B_2)	0 ± (≪1.0)
Total ± quadrature sum	−1.6 ± 2.1

the measured ratio [Eq. (5)] shifted by about 8 ppb suggesting that electrons are translated axially 3.3 μm from the position of the ion by an unintentional potential difference of ≃40 mV between the endcaps. Assuming that this shift in the ratio scales simply with B_1, the residual error in Eq. (5) from the reduced gradient should be ≪1 ppb. To test this, V_0 for electrons was doubled during our last four runs, but no statistically significant shifts in the result were observed.

Upon converting the ratio to the neutral carbon mass, Eq. (5) and the quadrature sum of the uncertainties from Table I yield the electron's atomic mass M_e = 0.000 548 579 911 1(12) u, with accuracy improved tenfold over the previously accepted value [1]. The total C^{6+} ionization energy 1105.864(4) nu used in this calculation is from Ref. [23] with unit conversion from Ref. [1]. Combining this result with the proton's atomic mass [13] yields the proton-electron mass ratio m_p/m_e = 1836.152 666 5(40), which agrees well with, and is an order of magnitude improvement over, previous determinations [1,10].

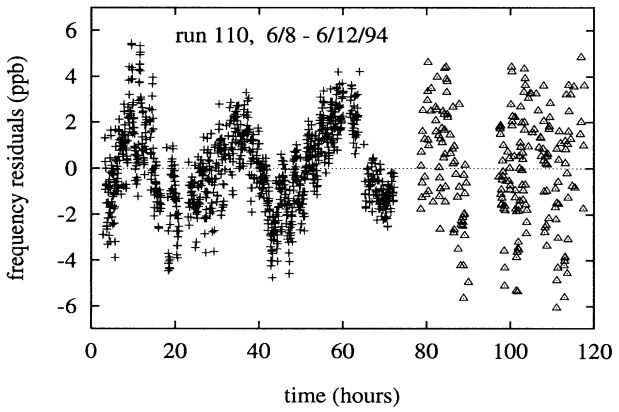

FIG. 4. Frequency residuals in parts per 10^9 after the ratio of cyclotron frequencies has been fit and a quadratic field drift removed from the data of a typical run. Here + and △ denote, respectively, single C^{6+} and electron cloud residuals.

We thank the National Science Foundation for their support of this work.

[1] E. R. Cohen and B. N. Taylor, Rev. Mod. Phys. **59**, 1121 (1987).
[2] B. N. Taylor (private communication).
[3] T. Andreae *et al.*, Phys. Rev. Lett. **69**, 1923 (1992).
[4] F. Nez *et al.*, Phys. Rev. Lett. **69**, 2326 (1992).
[5] M. Kasevich and S. Chu, Phys. Rev. Lett. **67**, 181 (1991).
[6] E. Krüger, W. Nistler, and W. Weirauch, Metrologia **32**, 117 (1995).
[7] G. Gärtner and E. Klempt, Z. Phys. A **287**, 1 (1978).
[8] G. Gräff, H. Kalinowsky, and J. Traut, Z. Phys. A **297**, 35 (1980).
[9] R. S. Van Dyck, Jr. and P. B. Schwinberg, Phys. Rev. Lett. **47**, 395 (1981).
[10] R. S. Van Dyck, Jr., F. L. Moore, D. L. Farnham, and P. B. Schwinberg, Int. J. Mass Spectrosc. Ion Proc. **66**, 327 (1985); Bull. Am. Phys. Soc. **31**, 244 (1986).
[11] G. Gabrielse *et al.*, Phys. Rev. Lett. **65**, 1317 (1990).
[12] D. J. Wineland, J. J. Bollinger, and W. M. Itano, Phys. Rev. Lett. **50**, 628 (1983).
[13] G. Audi and A. H. Wapstra, Nucl. Phys. **A565**, 1 (1993).
[14] R. S. Van Dyck, Jr., D. L. Farnham, and P. B. Schwinberg, in *Nuclei Far From Stability/Atomic Masses and Fundamental Constants, 1992*, edited by R. Neugart and A. Wöhr (Institute of Physics, Bristol, 1993), pp. 3–12.
[15] R. S. Van Dyck, Jr. D. L. Farnham, and P. B. Schwinberg, Phys. Scr. **46**, 257 (1992).
[16] R. S. Van Dyck, Jr., D. L. Farnham, and P. B. Schwinberg, J. Mod. Opt. **39**, 243 (1992).
[17] R. S. Van Dyck, Jr., D. J. Wineland, P. A. Ekstrom, and H. G. Dehmelt, Appl. Phys. Lett. **28**, 446 (1976).
[18] L. S. Brown and G. Gabrielse, Phys. Rev. A **25**, 2423 (1982).
[19] L. S. Brown and G. Gabrielse, Rev. Mod. Phys. **58**, 233 (1986).
[20] F. L. Moore *et al.*, Phys. Rev. A **46**, 2653 (1992).
[21] D. L. Farnham, Ph.D. thesis, University of Washington, 1995 (unpublished).
[22] R. S. Van Dyck, Jr., F. L. Moore, D. L. Farnham, and P. B. Schwinberg, Phys. Rev. A **40**, 6308 (1989).
[23] R. L. Kelly, J. Phys. Chem. Ref. Data **16**, 1 (1987).